Determination of Soil Erosion Risk in the Mustafakemalpasa River Basin, Turkey, Using the Revised Universal Soil Loss Equation, Geographic Information System, and Remote Sensing

Gokhan Ozsoy · Ertugrul Aksoy · M. Sabri Dirim · Zeynal Tumsavas

Abstract Sediment transport from steep slopes and agricultural lands into the Uluabat Lake (a RAMSAR site) by the Mustafakemalpasa (MKP) River is a serious problem within the river basin. Predictive erosion models are useful tools for evaluating soil erosion and establishing soil erosion management plans. The Revised Universal Soil Loss Equation (RUSLE) function is a commonly used erosion model for this purpose in Turkey and the rest of the world. This research integrates the RUSLE within a geographic information system environment to investigate the spatial distribution of annual soil loss potential in the MKP River Basin. The rainfall erosivity factor was developed from local annual precipitation data using a modified Fournier index: The topographic factor was developed from a digital elevation model; the K factor was determined from a combination of the soil map and the geological map; and the land cover factor was generated from Landsat-7 Enhanced Thematic Mapper (ETM) images. According to the model, the total soil loss potential of the MKP River Basin from erosion by water was 11,296,063 Mg year^{-1} with an average soil loss of 11.2 Mg year^{-1}. The RUSLE produces only local erosion values and cannot be used to estimate the sediment yield for a watershed. To estimate the sediment yield, sediment-delivery ratio equations were used and compared with the sediment-monitoring reports of the Dolluk stream gauging station on the MKP River, which collected data for >41 years (1964–2005). This station observes the overall efficiency of the sediment yield coming from the Orhaneli and Emet Rivers. The measured sediment in the Emet and Orhaneli sub-basins is 1,082,010 Mg year^{-1} and was estimated to be 1,640,947 Mg year^{-1} for the same two sub-basins. The measured sediment yield of the gauge station is 127.6 Mg km^{-2} year^{-1} but was estimated to be 170.2 Mg km^{-2} year^{-1}. The close match between the sediment amounts estimated using the RUSLE–geographic information system (GIS) combination and the measured values from the Dolluk sediment gauge station shows that the potential soil erosion risk of the MKP River Basin can be estimated correctly and reliably using the RUSLE function generated in a GIS environment.

Keywords Geographic information system · Remote sensing · Revised universal soil loss equation · Soil erosion modeling · Soil loss · Mustafakemalpasa river basin

Introduction

Human activities, such as mining, deforestation, construction, and agriculture, disturb natural land surfaces and lead to accelerated soil erosion, which is a serious problem worldwide and in Turkey (Oldeman 1991; Morgan 1995; van der Kniff and others 2000; Dogan 2002; Bayramin and others 2003; Wan 2003; Cerdan and others 2010). In the case of soil erosion, not only is the soil lost but the sediment also impairs the functioning and structural integrity of water reservoirs and dams.

Lakes are sensitive ecosystems and hotspots of human activity. Lake environments provide not only manmade landscapes, recreation areas for tourists, and a water reservoir for irrigation but also gathering places for migratory birds and habitats for millions of plants and animals.

G. Ozsoy (✉) · E. Aksoy · M. S. Dirim · Z. Tumsavas
Department of Soil Science and Plant Nutrition, Faculty of Agriculture, Uludag University, Gorukle Campus, Nilufer, Bursa 16059, Turkey
e-mail: ozsoygokhan@gmail.com

Uluabat Lake, which is the second biggest lake in the Bursa region, is one of the most important wetlands in Turkey; it is surrounded by wet meadows, especially on its northern and northwestern sides. Submerged plants cover almost all of the lake's shorelines, and the lake has the largest white water lily beds among Turkish wetlands. Due to its rich biodiversity, valuable freshwater sources, location along migratory bird routes, and position as an important breeding, feeding, and wintering site for significant bird populations, such as the globally threatened Dalmatian pelican and pygmy cormorant, Uluabat Lake was designated a RAMSAR (http://www.ramsar.org) site by the Turkish Ministry of Environment in 1998. It was also chosen as a partner in the International Living Lakes Network (http://www.globalnature.org) at the Fourth International Conference at EXPO 2000 (Aksoy and Ozsoy 2002; DHKD 2001).

According to Aksoy and Ozsoy (2002), Uluabat Lake covered an area of 133.1 km² in 1984, 120.5 km² in 1993, and 116.8 km² in 1998 based on multitemporal Landsat 5-Thematic Mapper (TM) imagery and aerial photographs. The approximately 12 % decrease in the area of Uluabat Lake between 1984 and 1998 is due to sediments transported by surface runoff from the irrigated agricultural areas and mining fields (commonly boron and marble quarries) in the surrounding catchment, particularly the Mustafakemalpasa (MKP) River catchment (Aksoy and Ozsoy 2002).

The MKP River Basin, where this study was conducted, has experienced significant landslide damage due to mining activities and progressive deforestation for agriculture, urbanization, and industry. Aksoy and Ozsoy (2002) reported that soil erosion was a critical issue at one study site on Uluabat Lake. According to Aksoy and Ozsoy (2002), the sediments carried and accumulated by the MKP River have a negative impact on the natural habitat of Uluabat Lake and threaten the existence of the lake. To understand Uluabat Lake's shrinking area, the soil erosion potential of the catchment should be determined. This study sought to determine this potential using the Revised Universal Soil Loss Equation (RUSLE) function. The RUSLE erosion model (Renard and others 1997) was chosen to assess erosion risk in the study area based on the available data, the purpose of the study, and the size of the watershed.

Predictive erosion models are useful tools for applying soil erosion and establishing soil erosion management plans. The RUSLE model (Renard and others 1997), a revised version of the Universal Soil Loss Equation (USLE) model (Wischmeier and Smith 1978), is the most widely used model for estimating the average annual soil loss from rill and sheet erosion both in Turkey and throughout the world (Chisci and Morgan 1988; Desmet

and Govers 1996; Millward and Mersey 1999; Dogan and others 2000; Dogan 2002; Angima and others 2003; Royall 2007; Ozcan and others 2008; Feng and others 2010). The USLE/RUSLE model is convenient and is compatible with the GIS (Hickey and others 1994; Jager 1994; Manoj and Kothyari 2000; Boggs and others 2001; Kinnel 2001, 2005; Suri and others 2002; Lee 2004; Lu and others 2004; Fu and others 2005; Lewis and others 2005; Onori and others 2006). Past research has showed that GIS and remote-sensing (RS) techniques are useful tools for estimating soil loss, especially given that the vegetation and land use and land cover (LULC) data derived from satellite imagery provide an economical method of modeling soil erosion (Cyr and others 1995; Wang and others 2003; de Jong 2006; Lee and Lee 2006; Pandey and others 2011).

Soil degradation in Turkey is an urgent issue (http://www.tema.org.tr/Sayfalar/CevreKutuphanesi/Turkiyede Erozyon.html [in Turkish; accessed: August 15, 2011]). Evaluating soil loss and determining the areas most vulnerable to soil erosion are necessary steps when promoting sustainable land use and comprehensive soil conservation management. This study integrates the RUSLE model with a GIS environment to investigate the spatial distribution of annual soil loss potential in the MKP River Basin to address Uluabat Lake's shrinking area. This study is the first attempt to produce a soil erosion map and to determine the areas of increased erosion risk in the studied catchment. It also proposes a new approach for generating the soil erodibility (K) factor in the RUSLE function when there is no detailed soil map. This approach is appropriate for Turkey and for other countries for which detailed soil maps are not available.

Materials and Methods

Study Site

The basin chosen as the study site lies between the latitudes 4,340,000 m and 4,455,000 m N and longitudes 618,000 m and 720,000 m E (UTM-ED50, Zone 35) and covers an area of 10,102 km² determined by a digital-elevation model (DEM) using the flow accumulation procedure of the Arc-Hydro tool developed for ArcGIS (ESRI [http://www.esri.com]) software. The DEM, a cell size of 20 m, was generated from contour vector data of 1:25.000 scale topographical maps with 10-m intervals. The location of the study area is shown in Fig. 1. According to the drainage network, this wide basin is composed of three main sub-basins: Emet (4,957 km²), Orhaneli (4,687 km²), and Mkp (458 km²). The bedrock geology of this area consists mainly of Neogen-aged terrestrial undifferentiated formations, serpentine, peridotite, pyroxenite, diorite, gabbros, and Paleozoic-aged
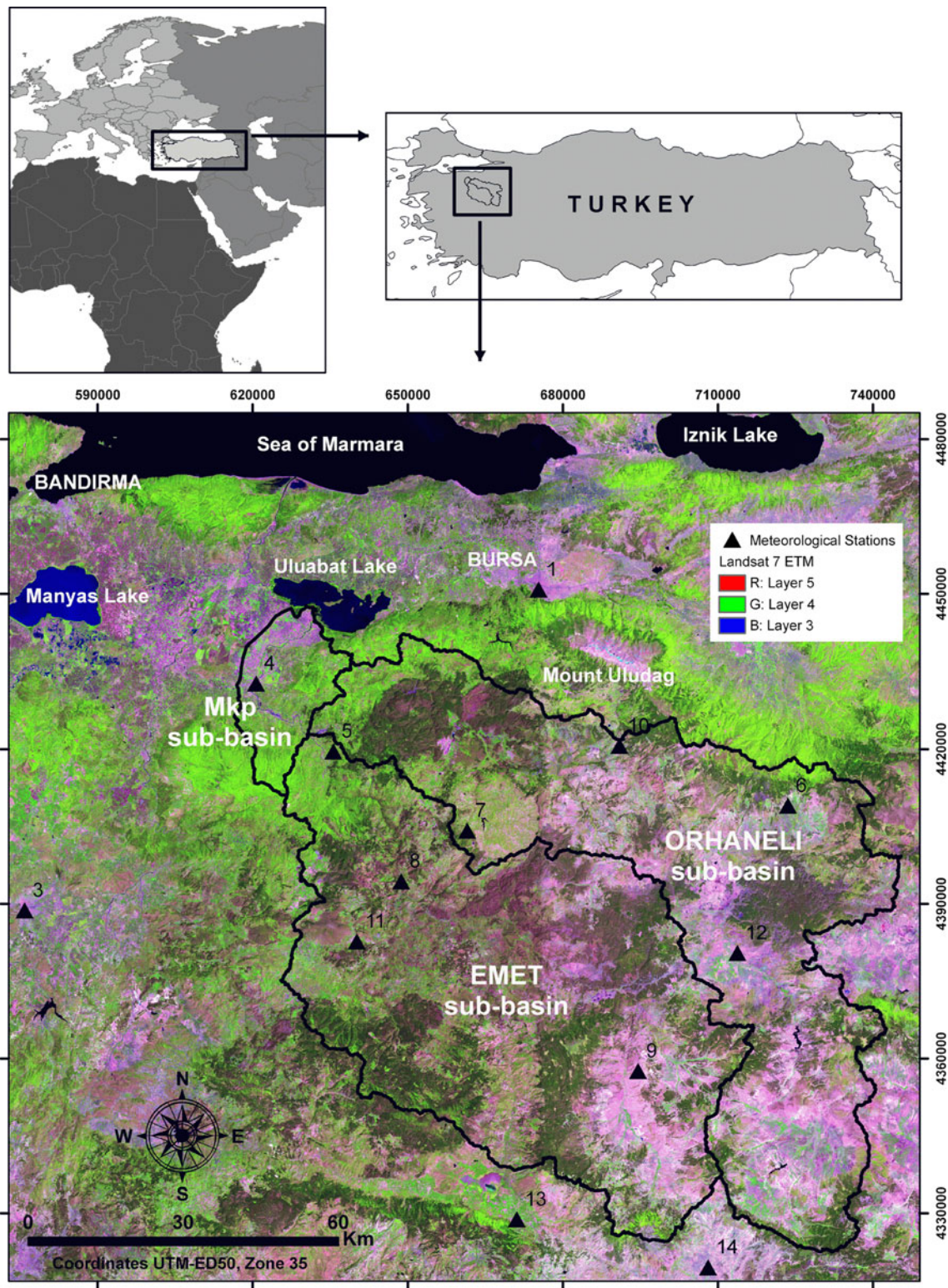
Fig. 1 The location map of the MKP River Basin and the meteorological stations used in the study

metamorphic rocks. The elevation in the basin ranges from 4 to 2,116 m above sea level. The upper part of the basin is mountainous, and the river forms deep valleys. The lower part of the basin is almost flat and forms an alluvial plain at the discharge point into Uluabat Lake. The climate in the basin is typical Mediterranean for the coastal lands of the Marmara

Fig. 2 Flowchart of the study for estimating soil loss using the RUSLE-GIS model
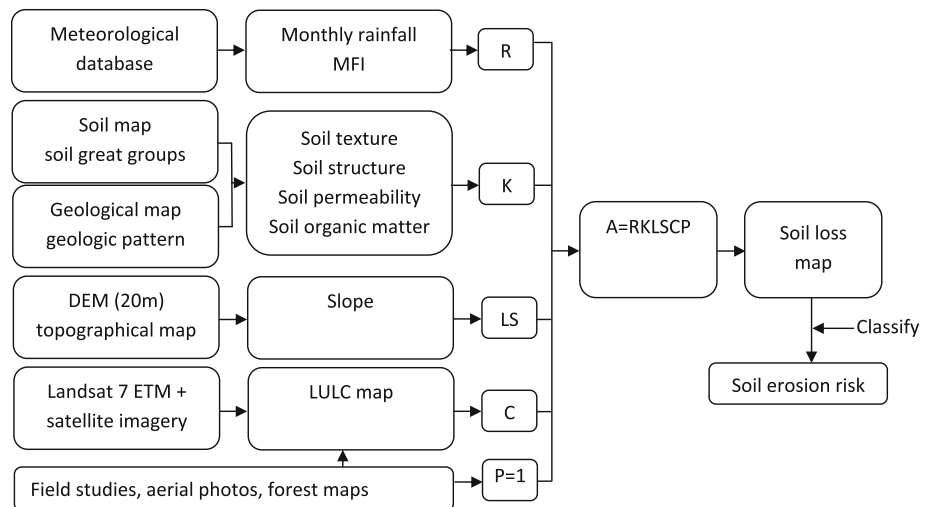
Sea. In the southeast parts and highlands of the basin, the climate is continental. The wet season begins in October and ends in May and followed by the dry season. The main precipitation in the basin is rain, which increases with elevation and changes to snow during the wet season in mountainous areas. The annual average precipitation in the basin ranges from 378.8 to 729 mm, and the mean temperature ranges from 9.5 to 14.5 °C (DMI 2006; Ozsoy 2007).

The soils of the basin are mainly composed of Non-Calcic Brown Forest Soils (49.5 %) and Brown Forest Soils (36.2 %). The distribution of the other soil types in the study area is as follows: Rendzinas (3.6 %), Alluvial (3.5 %), Colluvial (1.2 %), and Brown Soils (1 %). In addition, 5 % of the area is composed of water surface, construction sites, and bare rocks. The areas and ratios of the soil types were generated using GIS from 1:25,000 soil maps produced under the former United States classification system (1938 United States Department of Agriculture [USDA] soil classification system) and provided by the General Directorate of Rural Services of Turkey (KHGM). Unfortunately, these soil maps have not yet been updated using the modern soil taxonomy classification system.

The RUSLE Model

The USLE model consists of a set of calculations to estimate soil erosion in a plot of land with homogeneous characteristics (Wischmeier and Smith 1978). The RUSLE model retains the general framework of the USLE but refines the calculations for each of the five erosion factors with greater temporal and spatial detail (Renard and others 1997). With the RUSLE function, the average amount of soil loss is expressed as a function of five factors (Wischmeier and Smith 1965, 1978; Renard and others 1997) as follows:

$$A = R \times K \times LS \times C \times P \qquad (1)$$

where A is the computed average amount of soil loss in Mg ha^{-1} year^{-1}; R is the rainfall-runoff erosivity factor (MJ mm ha^{-1} h^{-1} year^{-1}); K is the soil erodibility factor (Mg ha h ha^{-1} MJ^{-1} mm^{-1}); LS is a combination of the slope length and steepness factors; C is the cover and management factor; and P is the support practices factor. LS, C, and P are dimensionless. The flowchart used to create the RUSLE-GIS soil erosion risk map and determine soil loss is shown in Fig. 2. The procedures to calculate the individual factors are described later in the text.

Rainfall Erosivity Factor

The rainfall erosivity (R) factor represents the effect of rainfall intensity on soil erosion and requires detailed, continuous data (Wischmeier and Smith 1978). In the RUSLE model, rainfall erosivity can be obtained by multiplying the total storm energy (E) and maximum 30-minute rainfall intensity (I_{30}) measurements for each rainstorm (Renard and others 1997). Unfortunately, these measurements are rarely available at standard meteorological stations in Turkey.

There are 14 meteorological stations established in and around the MKP River Basin as shown in Fig. 1, and the coordinate information of the meteorological stations is listed in Table 1. For most of these meteorological stations, the pluviograph and rainstorm data were particularly inadequate and unreliable for calculating the R factor in the RUSLE model. The general approach used to estimate the R factor when detailed pluviograph and rainstorm data are not available or reliable is to use the mean annual and monthly rainfall data from the meteorological stations located in the area under investigation (Arnoldus 1977, 1980; Renard and Freimund 1994; Lu and Yu 2002). To estimate the R factor using monthly and annual rainfall data, Arnoldus (1980) introduced a modified Fournier

Table 1 Meteorological stations used in the study and computed MFI and R factor values for each station

Meteorology station	Coordinates (UTM-ED50, Zone 35, meter)			MFI	R factor (MJ mm ha^{-1} h^{-1} year^{-1})
	Easting	Northing	Altitude		
Buyukorhan	661,477.9	4,404,238.5	810	41.4	513
Tavsanli	713,743.8	4,380,518.3	840	43.5	573
Emet	694,543.0	4,357,612.7	880	46.8	675
Harmancik	648,720.6	4,394,420.0	655	52.1	859
Kutahya	757,025.8	4,368,110.1	1,000	54.3	942
Dursunbey	640,126.1	4,382,757.0	600	57.8	1,084
Gediz	708,078.3	4,319,559.7	900	60.3	1,192
Balikesir	575,811.5	4,388,769.5	150	61.6	1,250
Devecikonagi	635,570.8	4,419,612.0	65	61.9	1,264
Domanic	723,523.7	4,409,097.4	880	65.3	1,425
Bursa	675,266.2	4,450,856.0	219	67.5	1,535
MKP	620,622.7	4,432,759.0	24	73.5	1,858
Keles	690,938.0	4,420,704.4	1,025	75.1	1,950
Simav	671,079.2	4,328,851.2	833	93.4	3,179

index (MFI) using the mean annual and monthly rainfall amount data:

$$\text{MFI} = \frac{\sum_{i=1}^{12}(\bar{p}i)^2}{\bar{P}} \qquad (2)$$

where $\bar{p}i$ is the mean rainfall amount (mm) for month i, and $\bar{P}$ is the mean annual rainfall amount (mm).

According to Arnoldus (1980), the MFI is a good approximation of the R factor (with which it is linearly correlated). For this study, long-term (from 1975 to 2005) precipitation data from 14 meteorological stations (with $\bar{P}$ ranging from 379 to 791 mm) located in and around the study area were collected, and the MFI was estimated for each station. To approximate the R factor using the calculated MFI for each station, the following R–MFI relationship, as suggested by Irvem and others (2007) for a climatologically similar (in terms of rainy days, amount, and range of precipitation distributed in the four seasons) basin in Turkey, was used as follows:

$$R = 0.1215 \times \text{MFI}^{2.2421} \qquad (3)$$

The MFI and R factor value of each meteorological station was estimated, and the R factor map of the MKP River Basin was produced with the Inverse Distance Weighted Average (IDW) interpolation method with a spatial resolution of 20×20 m in the GIS.

The IDW interpolation method is based on the assumption that the estimated value of a point is influenced more by nearby known points than those farther away (Weber and Englund 1992, 1994). In other words, the assigned weight is a function of inverse distance as represented in the following formula (Lam 1983).

$$f(x,y) = \frac{\left[\sum_{i=1}^{N} w(d_i)Z_i\right]}{\left[\sum_{i=1}^{N} w(d_i)\right]} \qquad (4)$$

where $f(x,y)$ is the interpolated value at point (x,y); $w(d_i)$ is the weighting function; z_i is the data value at point I; and di is the distance from point (x,y). The interpolated values of any point within the data set are bounded by $\min(z_i) < f(x,y) < \max(z_i)$ as long as $w(d_i) > 0$. The IDW interpolation method has been widely used on many types of data because of its simplicity in principle, speed in calculation, easiness in programming, and credibility in interpolating surfaces (Lam 1983).

Soil Erodibility Factor

The soil erodibility (K) factor is defined as the rate of soil loss per unit of R as measured on a unit plot, and it accounts for the influence of soil properties on soil loss during storm events. The K factor is related to soil texture, organic matter content, permeability class, and other factors, and it is largely determined by the soil type (Renard and others 1997).

According to the soil maps (scale 1:25,000) provided by the KHGM, the main soil types (great soil groups) in the basin are Non-Calcic Brown Forest Soils and Brown Forest Soils. These two great soil groups constitute 85.7 % of the basin, whereas 9.3 % is composed of Rendzinas, Alluvial, Colluvial, and Brown Soils. The remaining 5 % of the area is composed of water surface and bare rocks. Unfortunately, the available soil maps were old and insufficiently detailed for an accurate K assessment; the necessary information on soil structure class, fine texture, soil

permeability, and organic matter contents were inadequate. Without more detailed soil data, it is not possible to estimate the K factor in the RUSLE model.

Therefore, to obtain a more precise and accurate K factor, the soil maps were improved by generating a new soil map combining geological data (geological map scale 1:500,000) from the study area. The scale of the geological map was chosen because it was the only map produced that covered the entire basin. The geological map was scanned, digitized, and scaled to 1:25,000 to comply with the soil map (scale 1:25,000). After overlaying the soil map on the geological map, a new map was created that depicted every soil type formed on every different geological material.

Subsequently, every mapping unit that contained one of the great soil groups formed on various parent rocks was sampled. The number of samples was determined based on the coverage areas of the mapping units, and the samples were taken at a depth of 0–30 cm. Consequently, the number of the soil samples was increased by considering the geological pattern.

Using this new map, 168 soil samples were collected at each sampling site, and necessary information, such as slope, LULC type, soil structure, stoniness, and rockiness, was recorded as described by Schoeneberger and others (2002). Organic matter and soil texture were performed by laboratory analyses according to the Soil Survey Laboratory Methods Manual (Burt 2004). All of the soil information data were put into the attribute table of the soil map. For each soil mapping unit, a K factor was calculated using formulas (Wischmeier and Smith 1978) obtained from laboratory analysis results and on-site measurements as follows:

$$100 \times \text{K} = \left(2.1 \times 10^{-4}\right) \times (12 - \text{OM}) \times \text{M}^{1.14} \\ + 3.25 \times (\text{s} - 2) + 2.5 \times (\text{p} - 3) \,/\, \text{d} \quad (5)$$

$$\text{M} = (\% \text{ silt } + \% \text{ very fine sand}) \times (100 - \% \text{ clay}) \quad (6)$$

where OM is the organic matter (%); s is the soil structure class (1–6); p is the soil permeability class; M is the product of the primary particle size fraction; and d is the factor value for expressing K in SI units ($d = 7.59$).

Each soil type was associated with a K factor assuming that the same soil type has the same K factor throughout the study area. The K factor map was computed with the reclassification methods of the GIS.

Slope Length and Steepness Factor

The slope length and steepness (LS) factor accounts for the effect of topography on soil erosion (Renard and others 1997). Slope length is defined as the horizontal distance from the point of origin of the overland flow to the point where either the slope gradient decreases enough that deposition begins or runoff is concentrated in a defined channel (Wischmeier and Smith 1978). Slope steepness reflects the influence of slope gradient on erosion. An increase in the LS factor produces higher overland flow velocities and correspondingly greater erosion (Onori and others 2006).

The LS factor can be estimated from a DEM (Hickey and others 1994; Corwin and Wagenet 1996; Desmet and Govers 1996; Hickey 2000; Boggs and others 2001; Kinnel 2001; Gertner and others 2002; Wang and others 2003; van Remortel and others 2001, 2004). The DEM of the study area, a cell size of 20 m, was used to calculate the LS factor. The grid-based DEM was generated from contour vector data, which were digitized from 1:25,000-scale topographic maps with 10-m intervals. The maps were provided by the General Command of Mapping, Turkey. The DEM was produced with the "Topo to Raster" interpolation method in 3D Analyst tool of ArcGIS. "Topo to Raster" is an interpolation method specifically designed for the creation of hydrologically correct DEMs. It is based on the ANUDEM (version 4.6.3) program developed by Hutchinson (1989). See Hutchinson and Dowling (1991) for an example of a substantial application of ANUDEM and for additional associated references. A brief summary of ANUDEM and some applications are given in Hutchinson (1993).

To calculate the LS factor, a RUSLE-based Arc Macro Language (AML) program was adapted to generate an LS factor grid based on the 20-m DEM of the MKP River Basin. The algorithms in this procedure use the raster grid cumulation and maximum downhill slope methods. Specifically, the LS factor was estimated through an iterative slope length processing of the DEM data.

In the AML program, the RUSLE algorithms were used for calculating the L and S constituents after deriving the LS factor (van Remortel and others 2001). L is equal to (HPSL/RSL)^m, where HPSL is the horizontally projected slope length derived, and RSL is the 22.1-m reference slope length. For slopes of <9 % gradient, S is equal to $10.8 \times \sin(\text{slope\_angle}) + 0.03$; for slopes of ≥9 % gradient, S is equal to $16.8 \times \sin(\text{slope\_angle}) - 0.50$.

The AML program was developed by van Remortel and others (2001, 2004) and previously introduced by Hickey and others (1994) and is available at the following Web site with additional information: http://www.onlinegeographer.com/slope/slope.html (Accessed: October 10, 2011). Using this program, each 20-m cell of the grid surface of the study basin was assigned an LS value.

Land Cover and Management Factor

The land cover and management (C) factor is defined as the ratio of soil loss from land with specific vegetation to the

corresponding soil loss from continuous fallow (Wischmeier and Smith 1978). In this study, remotely sensed data have been used to estimate the C factor distribution based on LULC classification results (Millward and Mersey 1999; Reusing and others 2000), assuming that the same land covers have the same C factor values.

An LULC map of the MKP River Basin derived from the Landsat-7 Enhanced Thematic Mapper (ETM) full frame satellite images acquired on June 12, 2001 (route 179/32, row 179/33) and on May 18, 2001 (route 180/32, row 180/33), with a spatial resolution of 30-m, was used as the base map for determining the C factors. The digital image processing software ERDAS-Imagine (ERDAS Inc. [http://www.erdas.com]) was used to digitally interpret the satellite imagery. Reference data for classifying LULC in the study basin were collected from soil maps, aerial photographs, forest maps, and field studies. After synthesizing all of the information, the study area was classified into 10 LULC classes as follows: (1) broad-leaf forest, (2) coniferous forest, (3) sparse coniferous forest, (4) heathland, (5) pasture, (6) vineyard and fruit orchards, (7) complex cultivation pattern (agriculture), (8) fallow land (agriculture), (9) water body, and (10) bare rocks and construction sites. The supervised classification method (maximum likelihood) was used to extract the LULC classes as described by Lillesand and Kiefer (2000). The LULC classes and their areas are listed in Table 2. The C factors used in this study were adopted from previous studies (Canga 1995; Renard and others 1997; Yang and others 2003) that determined land classes using satellite data (Table 2).

The accuracy assessment is generally compiled in the form of a confusion matrix in which the columns depict the number of pixels per class for the reference data, and the rows show the number of pixels per class for the classified image. From this confusion matrix, a number of accuracy measures, such as the overall, the user's, and the producer's accuracy, can be determined. The overall accuracy is used to indicate the accuracy of the entire classification (i.e., the number of correctly classified pixels divided by the total number of pixels in the error matrix), whereas the other two measures indicate the accuracy of individual classes. The user's accuracy is regarded as the probability that a pixel classified on the map actually represents that class on the ground or reference data, whereas the producer's accuracy represents the probability that a pixel on reference data has been correctly classified (Stehman and Czaplewski 1998). In our case, the overall classification accuracy was found to be 92.1 %, whereas the user's accuracy and producer's accuracy were 89.3 %, and 92.6 %, respectively.

After creating the LULC map of the study basin, the C factors for the land classes were entered as attributes and a C factor map of the MKP River Basin was generated using the reclassification method in the GIS.

Support Practice Factor

The support practice (P) factor is the ratio of soil loss using a specific support practice to the corresponding loss with upslope and downslope tillage (Renard and others 1997). As in most agricultural lands in Turkey, agricultural practices in the study area consist of upslope and downslope tillage without any conservation support practices, such as contouring or terracing. This situation is evident in aerial photographs and land observations. To remove the P factor from the soil erosion estimates, P was set equal to one as suggested by Wischmeier and Smith (1978).

ArcGIS 9.1 software was used to generate the spatial distribution of the RUSLE factors. The four factor layers (R, K, LS, and C) were all converted into grids using a 20-m data set of the MKP River Basin in the same reference system. Subsequently, these grids were multiplied in

Table 2 LULC classes and C factors for the MKP River Basin

LULC class	C factor	MKP River Basin		Sub-basin cover ratio (%)		
		Area (km^2)	Ratio (%)	Mkp	Emet	Orhaneli
Broad-leaf forest	0.001	428	4.2	20.5	4.2	2.7
Coniferous forest	0.010	1,775	17.6	0.9	20.1	16.5
Sparsely coniferous forest	0.050	994	9.8	0.3	11.8	8.7
Heathland	0.038	2,647	26.2	20.6	26.6	26.4
Pasture	0.090	460	4.6	4.0	3.5	5.7
Vineyard and fruit orchards (agriculture)	0.180	104	1.0	2.3	0.9	1.0
Complex cultivation pattern (agriculture)	0.280	2,254	22.3	31.3	20.6	23.2
Fallow land (agriculture)	0.500	1,383	13.7	19.6	12.1	14.8
Water body	0.000	8	0.1	0.3	–	0.1
Bare rocks and construction sites	1.000	49	0.5	0.2	0.2	0.9
Total		10,102	100	100	100	100

the GIS as described by the RUSLE function. Thus, the annual soil loss was estimated on a pixel-by-pixel basis, and the spatial distribution of the soil erosion in the studied catchment was obtained.

Results and Discussion

Figure 3 shows the R factor map of the MKP River Basin. The average annual R factor ranged from 513 MJ mm ha^{-1} h^{-1} year^{-1} to 2,658 MJ mm ha^{-1} h^{-1} year^{-1}. The R values for the Mkp, Orhaneli, and Emet sub-basins ranged from 1,277 to 1,859, 513 to 1,951, and 567 to 2,658 MJ mm ha^{-1} h^{-1} year^{-1}, respectively. The computed MFI and R factor for each meteorological station are listed in Table 1. There was more rainfall erosivity in the north and northeast than in the south because rainfall erosivity is closely related to precipitation, which increases from south to north in the catchment (Fig. 3).
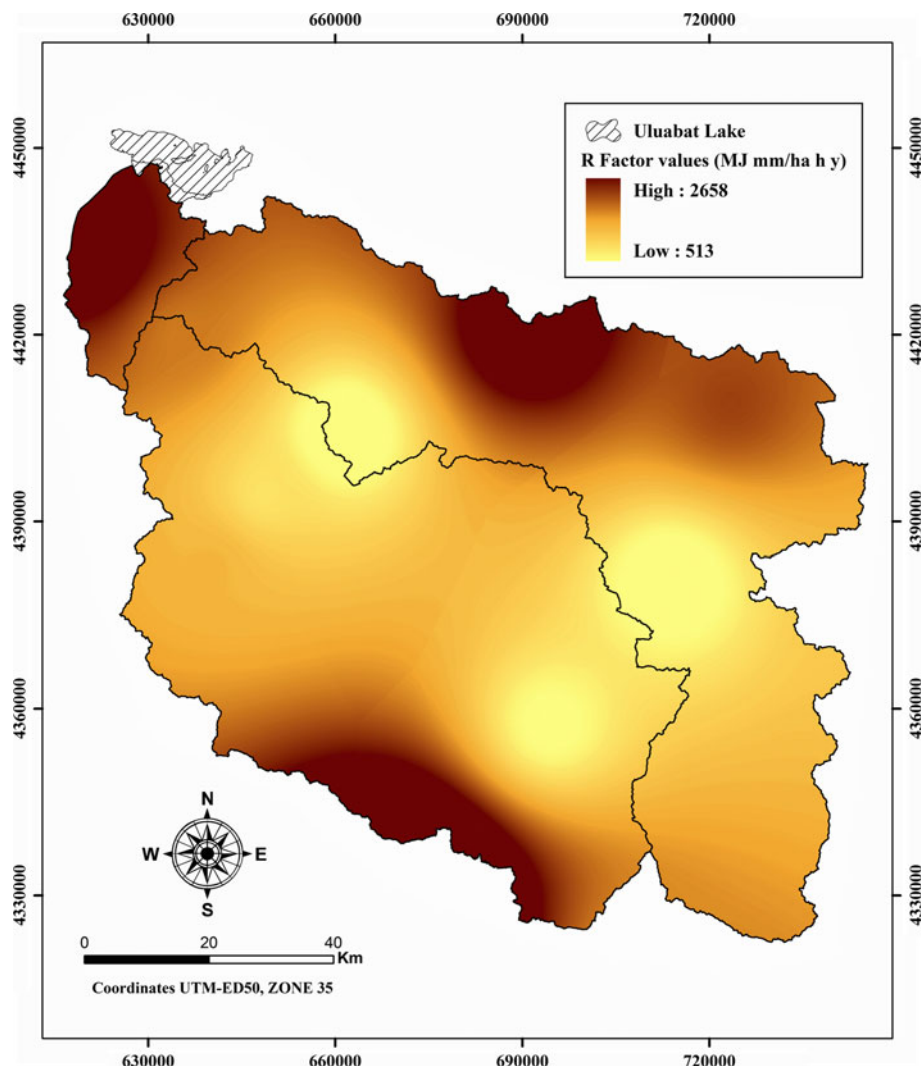
Figure 4 shows the map of the K factor, which varied from 1×10^{-4} to 5×10^{-2} Mg h MJ^{-1} mm^{-1}. The K factors were high in the northwest where the river has formed a delta (an alluvial plain) at the discharge point to Uluabat Lake. The K factors were also typically high in the eastern parts of the catchment on steep slopes where mostly medium and sandy textured soils occur.

Dogan and others (2000) studied the great soil groups (using the 1938 USDA soil classification system) of Turkey and reported their K factors. However, considering the soil map and the coverage area of the sites, the K factor of the six soil great groups previously mentioned insufficiently represent the study site because two of the six groups cover approximately 86 % of the area alone. If we had only used the information reported by Dogan and others (2000), the K factors would have been estimated from only six different soil mapping units over the wide basin, thus inaccurately estimating the K factor and leading to unrealistic results. Therefore, the soil maps must be more detailed to calculate the K factor accurately. Not only for this basin but also in

Fig. 3 The R factor map of the MKP River Basin (MJ mm ha^{-1} h^{-1} year^{-1})
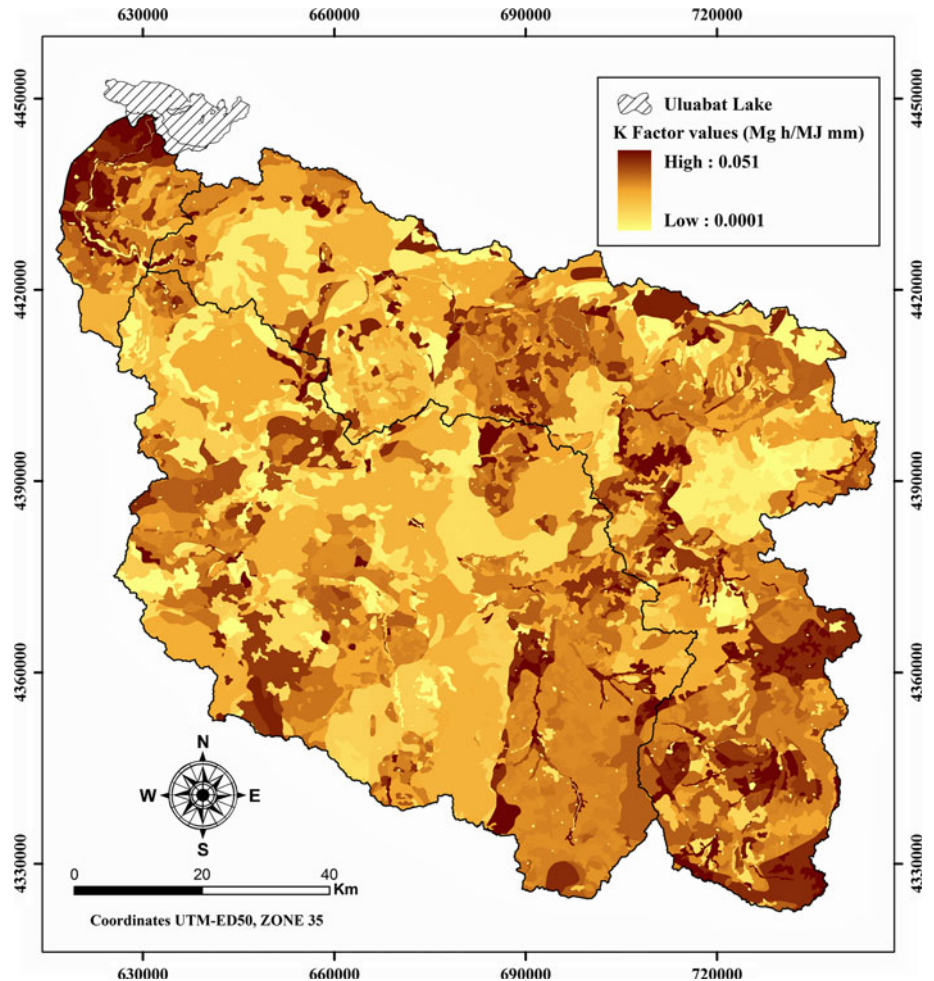
the rest of the country, more detailed soil maps have not been produced. Therefore, we generated a new map that is a combination of the soil map and the geological map of the basin in the GIS. Our approach of increasing the soil mapping units based on geological patterns produced more detailed information than the work of Dogan and others (2000), who originally introduced the K factors to describe the great soil groups in Turkey.

Figure 5 depicts the map of the LS factors, which ranged from 0.03 in the flat areas in the northwestern part of the basin to 70.07 in the high-lands (elevation approximately 2,000 m) in the northern, western, and southern parts of the basin, which had the steepest slopes, the greatest variability in elevation, and large LS values. The LS values were highest in the areas where the river forms deep valleys. These areas were mostly located in the upper part of the basin and also in the west and in the south.

Figure 6 shows the map of the C factor. This map was generated from the LULC map of the basin derived from satellite imagery. The area was found to be composed of 37 % agricultural lands, 31.6 % forests, 30.8 % heathland and pastures, and 0.6 % bare rocks, construction sites, and water bodies. The C factors ranged from 0 to 1.0 (Table 2) and were especially high in the northwestern and southeastern parts of the basin. In the northwest, the river formed an alluvial plain at the discharge point into Uluabat Lake, and the lands in this area are primarily used for agricultural production. In the southeastern parts of the basin, the C factors were also high because mining activities have brought progressive deforestation and increased amount of bare, exposed surfaces, which accelerate the loss of soil by erosion.

The spatial distribution of soil loss is listed in Table 3, and the soil loss map of the basin is shown in Fig. 7. The soil loss values ranged from 2×10^{-6} to 1,508 Mg ha^{-1} year^{-1}. The mean value of the soil loss was 11.2 Mg ha^{-1} year^{-1}. The total soil loss in the basin was 11,296,063 Mg year^{-1}. The maximum soil loss was in the Orhaneli sub-basin, which lost 11.3 Mg ha^{-1} year^{-1}. Soil loss values ranged between 4×10^{-6} and 1,374 Mg ha^{-1} year^{-1} for the Emet sub-basin, which had a mean value of 11.4 Mg ha^{-1} year^{-1}, and between 6×10^{-6} and 514 Mg ha^{-1} year^{-1} for the Mkp sub-basin, which had a mean value of 7.9 Mg ha^{-1} year^{-1}. The total soil losses for the Emet, Orhaneli, and Mkp sub-basins were

Fig. 5 The LS factor map of the MKP River Basin
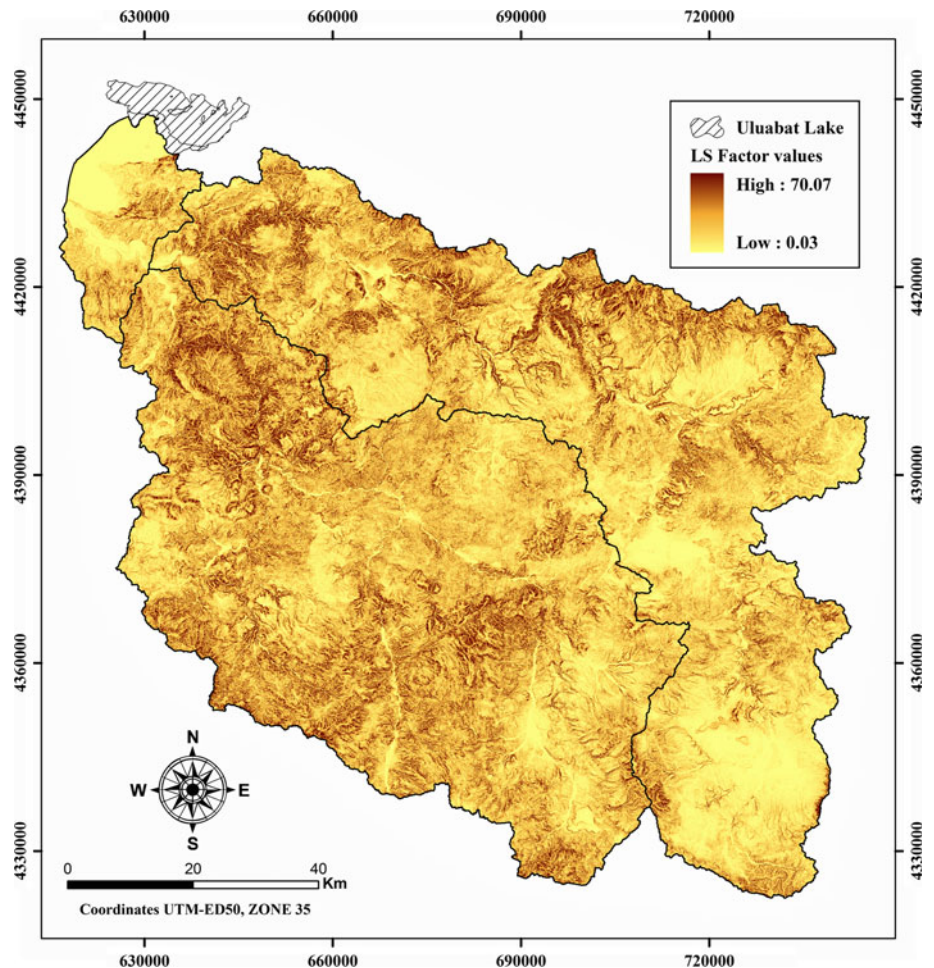
5,656,610 Mg year^{-1}, 5,278,343 Mg year^{-1}, and 361,110 Mg year^{-1}, respectively (Table 3).

The generated potential soil loss map of the study area was classified according to soil erosion risk (SER) classes to make a potential erosion risk classified map of the study basin. The potential risk classes and their distribution are listed in Table 4. More than half of the basin area was under low or low SER, and 25.9 % of the study area was under a high or high erosion risk. These amounts were 26.7 %, 25.7 %, and 19.4 % for the Emet, Orhaneli, and Mkp sub-basins, respectively (Table 4).

When the LULC and SER images are compared with each other, the relationship between the soil erosion and LULC classes may be more clearly understood. This comparison is valuable for understanding how different LULC classes affect soil erosion. Therefore, the LULC map and the SER map were compared pixel by pixel to generate a table indicating the relationship of the LULC and SER classes. Table 5 lists the percentage of SER with LULC classes. It indicates that forests (broad leaf and coniferous forests) have low erosion risk in the study area, but some of the cultivated and fallow agricultural areas

have high or very high erosion risks. The importance of the P factor occurs in these areas. The P factor should be developed in agricultural areas to decrease soil erosion to an acceptable limit. However, in flat or almost flat areas, where agriculture is the main land use type, the erosion risk was found to be low. Table 5 also lists that some areas of sparse coniferous forests, heathlands, and pastures had high or medium erosion risks, whereas most of them have low risk. To decrease the soil erosion in these lands, sparse forests, heathlands, and pastures with limited ground cover should be improved and managed well. Thus, a major part of these lands may be protected from erosion. In addition, the other land covers, such as bare rocks and construction sites, occurred in all risk classes, but few of them had very low risk, and 77.6 % of them had very high erosion risk (Table 5).

The Mediterranean region is particularly prone to erosion because it is subject to long, dry periods fallowed by heavy bursts of rainfall that falls on steep slopes with fragile soils, resulting in considerable amounts of erosion (van der Kniff et al. 2000). The erosion rates in this study are quite low for a Mediterranean region. This might be

Fig. 6 The C factor map of the MKP River Basin
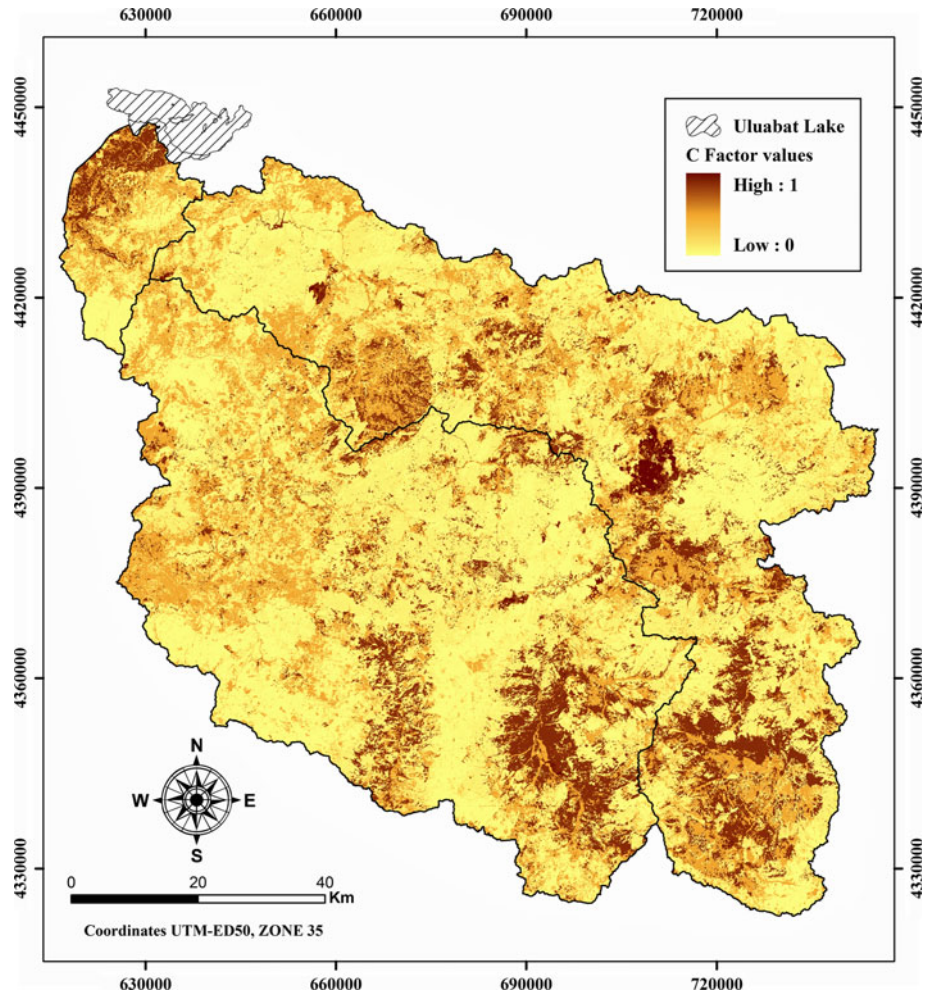
Table 3 Aggregate distribution of soil loss for the MKP River Basin and its sub-basins

Watersheds	Area (km^2)	Minimum soil loss (Mg ha^{-1} year^{-1})	Maximum soil loss (Mg ha^{-1} year^{-1})	Mean soil loss (Mg ha^{-1} year^{-1})	Total soil loss (Mg year^{-1})
Mkp	458	6×10^{-6}	514	7.9	5,656,610
Emet	4,957	4×10^{-6}	1,374	11.4	5,278,343
Orhaneli	4,687	2×10^{-6}	1,508	11.3	361,110
MKP River Basin (total)	10,102	2×10^{-6}	1,508	11.2	11,296,063

due to gully erosion, which cannot be predicted using the RUSLE model, being the main type of erosion in the area. Another reason for the overall low erosion rates could be the C factor. Even though a large portion of the area is bare, there are some patches of dense maquis-like vegetation that would be expected to show much higher C values. Furthermore, in some mountainous areas at the northern and southern parts of the basin, the erosion process is highly influenced both by its LS and high R values. However, these factors are effectively opposed by forest cover. Special priority must be given to the protection of natural forests and pasturelands, especially on steep slopes.

In agricultural lands, crop rotation and appropriate soil tillage practices must be used to increase plant coverage and decrease the loss of soil by erosion.

The RUSLE function estimates only local erosion amounts and cannot be used to estimate the sediment yield for an entire watershed (Renard and others 1997). For this purpose, sediment delivery ratio (SDR) equations were used and compared with the sediment monitoring reports of the Dolluk stream gauging station along the Mustafake-malpasa River.

Lim and others (2003) tested SDR curves for 300 different basins and found support for Vanoni's (1975) SDR

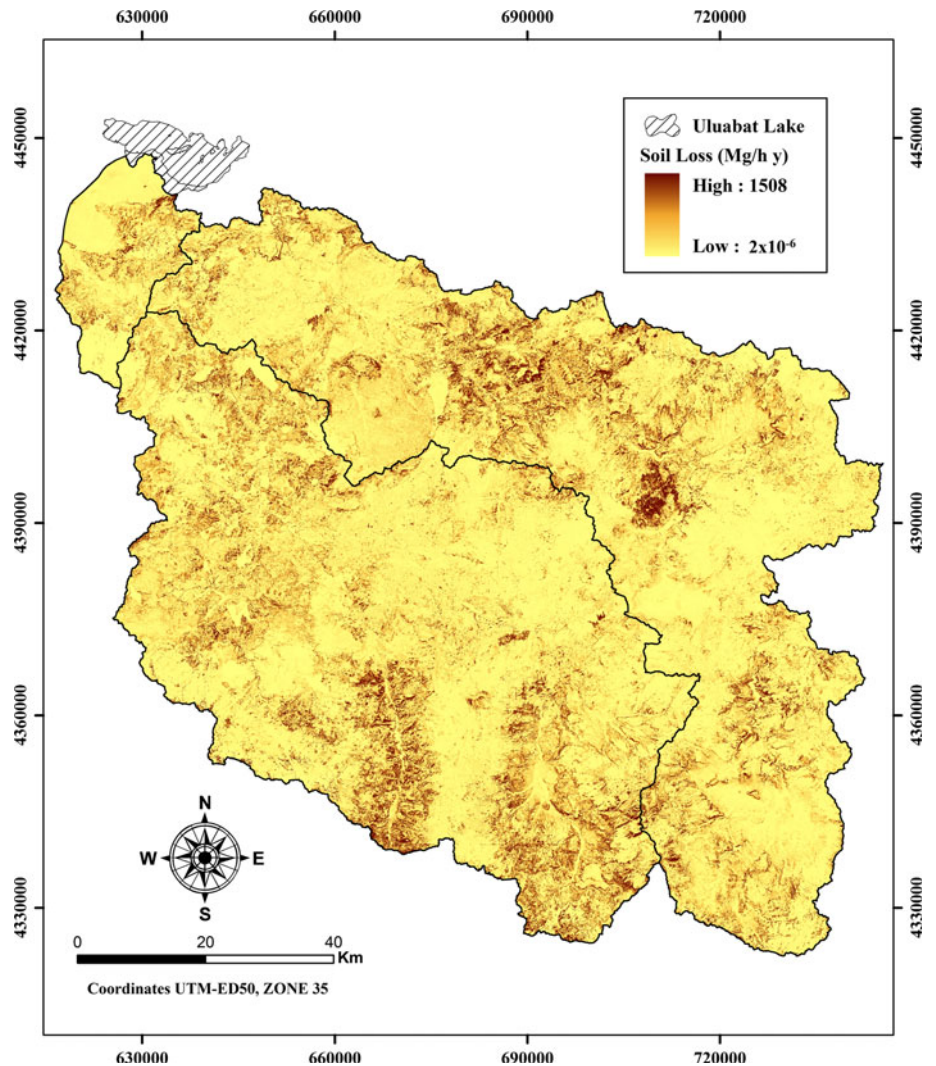**Fig. 7** The soil loss map of the MKP River Basin (Mg ha^{-1} year^{-1})

Table 4 SER classes for the MKP River Basin and its sub-basins

Soil loss (Mg ha^{-1} year^{-1})	SER class	MKP River Basin		Sub-basin (area [%])		
		Area (km^2)	Area (%)	Mkp	Emet	Orhaneli
0–3	Very low	5,044	49.9	63.6	48.2	50.4
3–5	Low	1,078	10.7	7.6	11.2	10.4
5–10	Moderate	1,365	13.5	9.4	13.9	13.5
10–20	High	1,085	10.7	7.7	10.8	11.0
>20	Very high	1,530	15.2	11.7	15.9	14.7
	Total	10,102	100	100	100	100

curve using the Sediment Assessment Tool for Affective Erosion Control (SATEEC) (http://www.envsys.co.kr/~sateec/) modeling software. The annual sediment and yield of the MKP River Basin and its sub-basins were calculated using a SDR curve, developed by Vanoni (1975), as follows:

$$SDR = 0.4724\, A^{-0.125} \qquad (7)$$

where A is the area of the basin (km^2).

The SDR results are listed in Table 5. The amount of sediment arriving at Uluabat Lake was calculated by the SDR, and the SDR was also useful for verifying the results obtained from the RUSLE-GIS function.

In addition, 41 years (1964–2005) of sediment amount and yield data (EIE 2000, 2005) from the Dolluk sediment gauge station were collected for comparison with the estimates from the RUSLE function. This station observes the overall efficiency of the sediment yield coming from the Orhaneli and Emet Rivers. The measured sediment in the Emet and Orhaneli sub-basins is 1,082,010 Mg year^{-1} and was estimated to be 1,640,947 Mg year^{-1} for the same two sub-basins using the Vanoni (1975) approach. The measured sediment yield of the gauge station is 127.6 Mg km^{-2} year^{-1}, but it was estimated to be 170.2 Mg km^{-2} year^{-1} using the Vanoni (1975) function

Table 5 Assessment of SER and associated land cover distribution for the MKP River Basin

LULC class	SER (%)				
	Very low	Low	Moderate	High	Very high
Forest (broad-leaf, coniferous)	95.3	3.9	0.8	–	–
Sparsely coniferous forest	43.9	20.2	23.5	10.3	2.1
Heathland	57.7	17.7	17.5	6.2	0.9
Pasture	39.7	15.7	21.8	15.6	7.2
Agriculture (orchards, cultivated, fallow)	21.0	6.7	14.7	19.8	37.8
Bare rocks and construction sites	8.3	1.3	3.8	9.0	77.6

Table 6 Estimated and measured sediment amounts and yield for the MKP River Basin and its sub-basins

Sub-basin	Area (km^2)	Soil loss (Mg year^{-1})	Sediment delivery ratio (Vanoni 1975)	Estimated (Vanoni 1975)		Measured (EIE 2000, 2005)	
				Sediment amount (Mg year^{-1})	Sediment yield (Mg km^{-2} year^{-1})	Sediment amount (Mg year^{-1})	Sediment yield (Mg km^{-2} year^{-1})
Mkp	458	361,110	0.22	79,312	173.2	–	–
Emet	4,957	5,656,610	0.16	922,494	186.1	–	–
Orhaneli	4,687	5,278,343	0.16	866,853	184.9	–	–
Orhaneli and Emet	9,644	10,934,953	0.15	1,640,947	170.2	1,082,010	127.6
MKP River Basin (total)	10,102	11,296,063	0.15	1,685,334	166.8	–	–

(Table 6). The close match between the sediment amounts estimated using the RUSLE-geographic information system (GIS) function and the measured values from the Dolluk sediment gauge station shows that the potential soil erosion risk of the MKP River Basin can be estimated correctly and reliably using the RUSLE function generated in the GIS.

Despite the deficiencies and shortcomings discussed previously, the method used produced valuable information on SER. The main value of this spatial analysis is to identify areas that are vulnerable to soil erosion. This can be helpful when taking necessary actions to overcome the erosion problem. However, further analysis of the R, C, and P factors could improve the results and the model's efficiency. The LS factor and spatial resolution used in this analysis are sensitive enough to estimate soil loss using the RUSLE model. The method was found to be relatively simple and has a wide range of applicability.

Conclusion

The RUSLE model was applied to estimate soil loss using RS and GIS in the MKP River Basin located in the

northwest part of Turkey. This is an effective way to map the spatial distribution of SER in a large area.

Detailed pluviograph data for calculating the R factor was not available. Therefore, the R factor was estimated using a regression formula developed for a similar Mediterranean region in Turkey using calculated MFI data based on mean annual and monthly rainfall data from the meteorological stations located in and around the study area. Given the soil data available, the inadequate K factor data were improved by generating a new soil map by combining the existing data with field surveys and geological mapping data from the study area. The LS factor was estimated using a GIS-automated hydrologic procedure to calculate the slope length and steepness. The C factors were determined from the LULC map of the study area, which was derived from satellite images, and the borders of the LULC types were checked and corrected using aerial photographs and forest maps. In this study, the P factor was assumed to be 1, meaning that soil conservation support practices were not present in the studied area. This reality was observed in field studies as well a aerial photographs of the basin.

The average soil loss was 11.2 Mg ha^{-1} year^{-1} in the basin. More than half of the basin was found to be under low or very low water erosion risk. This was primarily

because the R and C factors did not predict high soil loss in the basin. However, because of the progressive deforestation and agriculture, approximately 26 % of the study area was under high or very high erosion risk.

The values, as estimated using the RUSLE model, were consistent with the measured values obtained from the Dolluk sediment gauge station. This shows that the RUSLE model can be efficiently applied at the basin scale with modest data requirements. Despite the deficiencies and shortcomings discussed in the previous section, the method has produced valuable information on SER with limited data. However, improved estimates of the R, C, and P factors could improve the results and the model's efficiency.

We were able to estimate erosion rates in the studied area by overlaying the soil map on a geological map, thus creating a joint map. This approach can be used in regions where a detailed soil map is not available. This approach can also be used to determine the areas most sensitive to soil erosion, which would allow the development of sustainable land use plans and the implementation of comprehensive soil conservation management.

References

Aksoy E, Ozsoy G (2002) Investigation of multi-temporal land use/cover and shoreline changes of the Uluabat Lake RAMSAR Site using RS and GIS. In: *Proceedings of the International Conference On Sustainable Land Use and Management, June 10-13*. Soil Science Society of Turkey and the Scientific and Technological Research Council of Turkey, Canakkale, Turkey, pp 318–325

Angima SD, Stott DE, O'Neill MK, Ong CK, Weesies GA (2003) Soil erosion prediction using RUSLE for central Kenyan highland conditions. Journal of Agriculture, Ecosystems, and Environment 97:295–308

Arnoldus HMJ (1977) Methodology used to determine the maximum potential average annual soil loss due to sheet and rill erosion in Morocco. FAO Soils Bulletin 34:39–51

Arnoldus HMJ (1980) An approximation of the rainfall factor in the universal soil loss equation. In: De Boodt M, Gabriels D (eds) Assessment of erosion. Wiley, Chichester, pp 127–132

Bayramin I, Dengiz O, Baskan O, Parlak M (2003) Soil erosion risk assessment with ICONA model, case study: Beypazari area. Turkish Journal of Agriculture and Forestry 27:105–116

Boggs G, Devonport C, Evans K, Puig P (2001) GIS-based rapid assessment of erosion risk in a small catchment in the wet/dry tropics of Australia. Land Degradation and Development 12:417–434

Burt R (ed) (2004) *Soil survey laboratory methods manual*. Soil Survey Investigations Report No. 42, Version 4.0. United States Department of Agriculture–Natural Resources Conservation Service. United States Government Printing Office, Washington, DC

Canga MR (1995) *Soil and water conservation* (in Turkish). Press No. 1386. Ankara University, Faculty of Agriculture, Ankara, pp 43–64

Cerdan O, Govers G, Le Bissonnais Y, Van Oost K, Poesen J, Saby N et al (2010) Rates and spatial variations of soil erosion in Europe: A study based on erosion plot data. Geomorphology 122:167–177

Chisci C, Morgan RPC (1988) Modeling soil erosion by water: Why and how? In: Dino T (ed) *Agriculture erosion assessment and modeling*. EU pp 123–145

Corwin DL, Wagenet RJ (1996) Application of GIS to the modeling of non-point source pollutants in the Vadoze Zone: A conference overview. Journal of Environmental Quality 25(3):403–411

Cyr L, Bonn F, Pesant A (1995) Vegetation indices derived from remote sensing for an estimation of soil protection against soil erosion. Ecological Modeling 79:277–285

de Jong SM (2006) Derivation of vegetative variables from Landsat TM for modeling soil erosion. Earth Surface Process and Landforms 19(2):165–178

Desmet PJJ, Govers G (1996) A GIS procedure for automatically calculating the USLE-LS factor on topographically complex landscape units. Journal of Soil and Water Conservation 51(5):427–435

DHKD (2001) *Uluabat Lake management plan* (draft report [in Turkish]). Turkish Ministry of Environment and Society of Natural Life Protection, Ankara

DMI (2006) Multiyear annual and monthly precipitation and temperature data reports for the meteorological stations: Bursa, Mustafakemalpasa, Keles, Buyukorhan, Harmancik, Balikesir, Dursunbey, Domanic, Kutahya, Emet, Gediz, Simav, Devecikonagi, Tavsanli (in Turkish). Republic of Turkey, Ministry of Environment and Forestry, Meteorological Service of Turkey, Turkey

Dogan O (2002) *Erosive potentials of rainfalls in Turkey and erosion index values of universal soil loss equation* (in Turkish). Publication No. 220, Report No. R-120. Publication of Ankara Research Institute, General Directorate of Rural Service, Ankara

Dogan O, Cebel H, Kucukcakar N, Akgul S (2000) *The erodibility factor for the great soil groups in Turkey* (in Turkish). Publication No. 111, Report No. 17. General Directorate of Rural Services of Turkey Research Planning and Coordination Unit, Soil and Water Resources Research Directorate, Ankara

EIE (2000) *Suspended sediment data and sediment transport amounts for surface waters in Turkey, part 3: Susurluk Basin* (in Turkish). Publication No. 20-17. Republic of Turkey, General Directorate of Electrical Power Resources Survey and Development Administration, Ankara, pp 24–59

EIE (2005) *Multiyear suspended sediment data and sediment transport amounts for Dolluk station (no. 302) at Mustafakemalpasa River* (in Turkish). Republic of Turkey, General Directorate of Electrical Power Resources Survey and Development Administration, Ankara

Feng X, Wang Y, Chen L, Fu B, Bai G (2010) Modeling soil erosion and its response to land-use change in hilly catchments of the Chinese Loess Plateau. Geomorphology 118:239–248

Fu BJ, Zhao WW, Chen LD, Zhang QJ, Lu YH, Gulinck H, Poesen J (2005) Assessment of soil erosion at large watershed scale using RUSLE and GIS: A case study in the Loess Plateau of China. Land Degradation and Development 16:73–85

Gertner G, Wang G, Fang S, Anderson AB (2002) Effect and uncertainty of digital elevation model spatial resolutions on predicting the topographical factor for soil loss estimation. Journal of Soil and Water Conservation 57(3):164–182

Hickey R (2000) Slope angle and slope length solutions for GIS. Cartography 29:1–8

Hickey R, Smith A, Jankowski P (1994) Slope length calculations from a DEM within ArcInfo GRID. Computing, Environment and Urban Systems 18(5):365–380

Hutchinson MF (1989) A new procedure for gridding elevation and stream line data with automatic removal of spurious pits. Journal of Hydrology 106:211–232

Hutchinson MF (1993) Development of a continent-wide DEM with applications to terrain and climate analysis. In: Goodchild MF et al (eds) Environmental modeling with GIS. Oxford University Press, New York, pp 392–399

Hutchinson MF, Dowling TI (1991) A continental hydrological assessment of a new grid-based digital elevation model of Australia. Hydrological Processes 5:45–58

Irvem A, Topaloglu F, Uygur V (2007) Estimating spatial distribution of soil loss over Seyhan River Basin in Turkey. Journal of Hydrology 336:30–37

Jager S (1994) Modeling regional soil erosion susceptibility using the universal soil loss equation and GIS. In: Rickson RJ (ed) Conserving soil resources: European perspectives. CAB International, Wallingford, pp 161–177

Kinnel PIA (2001) Slope length factor for applying the USLE-M to erosion in grid cells. Soil Tillage Research 58:11–17

Kinnel PIA (2005) Alternative approaches for determining the USLE-M slope length factor for grid cells. Soil Science Society of America Journal 69:674–680

Lam NSN (1983) Spatial interpolation methods: a review. American Cartographer 10(2):129–149

Lee S (2004) Soil erosion assessment and its verification using the universal soil loss equation and geographic information system: a case study at Boun, Korea. Environmental Geology 45:457–465

Lee GS, Lee HS (2006) Scaling effect for estimating soil loss in the RUSLE model using remotely sensed geospatial data in Korea. Hydrology and Earth System Sciences Discussions 3:135–157

Lewis LA, Verstraeten G, Zhu H (2005) RUSLE applied in a GIS framework: calculating the LS factor and deriving homogeneous patches for estimating soil loss. International Journal of Geographic Information Science 19(7):809–829

Lillesand TM, Kiefer RW (2000) Remote sensing and image interpretation (4th ed). Wiley, New York

Lim KJ, Choi J, Kim K, Sagong M, Engel BA (2003) Development of sediment assessment tool for affective erosion control (SATEEC) in small scale watershed. Transactions of the Korean Society of Agricultural Engineers 45(5):85–96

Lu H, Yu B (2002) Spatial and seasonal distribution of rainfall erosivity in Australia. Australian Journal of Soil Research 40(6):887–901

Lu D, Li G, Valladares GS, Batistella M (2004) Mapping soil erosion risk in Rondonia, Brazilian Amazonia: using RUSLE, remote sensing and GIS. Land Degradation and Development 15:499–512

Manoj KJ, Kothyari UC (2000) Estimation of soil erosion and sediment yield using GIS. Hydrological Sciences 45(5):771–786

Millward AA, Mersey JE (1999) Adapting the RUSLE to model soil erosion potential in a mountainous tropical watershed. Catena 38:109–129

Morgan RP (1995) Soil erosion and conservation (2nd ed). Longman Group, Cranfield

Oldeman LR (1991) Global extent of soil degradation. Bio-annual report. International Soil Reference and Information Center, Waganingen, The Netherlands, pp 19–36

Onori F, De Bonis P, Grauso S (2006) Soil erosion prediction at the basin scale using the revised universal soil loss equation

(RUSLE) in a catchment of Sicily (southern Italy). Environmental Geology 50:1129–1140

Ozcan AU, Erpul G, Basaran M, Erdogan HE (2008) Use of USLE/GIS technology integrated with geostatistics to assess soil erosion risk in different land uses of Indagi Mountain Pass-Cankiri, Turkey. Environmental Geology 53:1731–1741

Ozsoy G (2007) Determination of the potential erosion risk using remote sensing (RS) and geographic information system (GIS) techniques (in Turkish). Doctoral thesis, Uludag University, Bursa

Pandey A, Chowdary VM, Mal BC, Dabral PP (2011) Remote sensing and GIS for identification of suitable sites for soil and water conservation structures. Land Degradation and Development 22:359–372

Renard KG, Freimund JR (1994) Using monthly precipitation data to estimate the R-factor in the revised USLE. Journal of Hydrology 157:287–306

Renard KG, Foster GR, Weesies GA, McCool DK, Yoder DC (1997) Predicting soil erosion by water: A guide to conservation planning with the Revised Universal Soil Loss Equation (RUSLE). Agricultural Handbook No 703. United States Department of Agriculture, Washington, DC

Reusing M, Schneider T, Ammer U (2000) Modeling soil erosion rates in the Ethiopian Highlands by integration of high resolution MOMS-02/D2-stereo-data in a GIS. International Journal of Remote Sensing 21:1885–1896

Royall D (2007) A comparison of mineral-magnetic and distributed RUSLE modeling in the assessment of soil loss on a southeastern US cropland. Catena 69:170–180

Schoeneberger PJ, Wysocki DA, Benham EC, Broderson WD (eds) (2002) Field book for describing and sampling soils, version 2.0. National Soil Survey Center, United States Department of Agriculture–Natural Resources Conservation Service, Lincoln

Stehman SV, Czaplewski RL (1998) Design and analysis for thematic map accuracy assessment: Fundamental principles. Remote Sensing of Environment 64:331–344

Suri M, Cebecauer T, Hofierka J, Fulajtar E (2002) Erosion assessment of Slovakia at a regional scale using GIS. Ecology (Bratislava) 21(4):404–422

van der Kniff JM, Jones RJA, Montanarella L (2000) Soil erosion risk assessment in Italy. European Commission Directorate General, Joint Research Centre Space Applications Institute and European Soil Bureau. EUR 19022EN. Italy

van Remortel RD, Hamilton ME, Hickey RJ (2001) Estimating the LS factor for RUSLE through iterative slope length processing of digital elevation data within ArcInfo Grid. Cartography 30(1):27–35

van Remortel RD, Maichle RW, Hickey RJ (2004) Computing the LS factor for the revised universal soil loss equation through array-based slope processing of digital elevation data using C++ executable. Computers and Geosciences 30(9–10):1043–1053

Vanoni VA (1975) Sedimentation engineering, manual and reports on engineering. Practice No. 54. American Society of Civil Engineers, New York

Wan J (2003) Land degradation and ecological rehabilitation in karst areas of Guizhou Province, southwestern China. Advances in Earth Sciences 3:447–453

Wang G, Gertner G, Fang S, Anderson AB (2003) Mapping multiple variables for predicting soil loss by geostatistical methods with TM images and a slope map. Photogrametric Engineering and Remote Sensing 69:889–898

Weber D, Englund EJ (1992) Evaluation and comparison of spatial interpolators. Mathematical Geology 24(4):381–391

Weber D, Englund EJ (1994) Evaluation and comparison of spatial interpolators—II. Mathematical Geology 26(5):589–603

Wischmeier WH, Smith DD (1965) Predicting rainfall erosion losses from cropland east of the Rocky Mountains: Guide for selection of practices for soil and water conservation. Agriculture Handbook No. 282. United States Department of Agriculture, Washington, DC

Wischmeier WH, Smith DD (1978) Predicting rainfall erosion losses: A guide to conservation. Agricultural Handbook No. 537.

Planning, Science and Education Administration. United States Department of Agriculture, Washington, DC

Yang D, Kanae S, Oki T, Koikel T, Musiake T (2003) Global potential soil erosion with reference to land use and climate change. Hydrological Processes 17(14):2913–2928